

Customized and Optimized Treatment of Extended-Spectrum-Beta-Lactamase Bacteria for Individual Patients

Irene Yicheng Jiang^{1,*} and Will Cao²

¹ Concord Academy, Massachusetts, United States

² Duke University, Durham, United States

Email: irenejiangyc@gmail.com (I.Y.J.); caoyxl@gmail.com (W.C.)

*Corresponding author

Abstract—This paper discusses the optimization of customized intravenous-drip therapy regimens for individual patients infected with antibiotic-resistant bacteria, namely Extended-Spectrum-Beta-Lactamase (ESBL) bacteria. By utilizing Ordinary Differential Equations (ODE) to model the system's dynamics, evaluated the efficiencies of the four most typical types of pulse functions, namely Dirac delta, sine, trapezoid, and normal distribution functions, as well as the time required for each treatment to suppress the pathogen population. The results revealed that a trapezoid pulse function for intravenous delivery of antibiotics is most favorable. Subsequently, infection severity was randomized by altering the bacterial and Beta-Lactamase population. The efficiency of each randomized regimen was evaluated using a predetermined score matrix that assessed the dosing length, dosing interval, maximum rate of antibiotic infusion, net consumption of antibiotics, and the total number of required treatments. Radar charts and box plot models were employed to present the findings. It was discovered that for more severely infected patients with a higher initial population and growth rate, it is important to decrease the time interval between subsequent doses and increase the time of maximum infusion rate. Conversely, for mild infections, the time interval between doses should be increased, and the time of maximum infusion rate should be decreased. It should be noted that maximizing the infusion rate does not enhance treatment efficiency. Furthermore, in comparison to the initial infected bacteria population size, the growth rate, and Bla production rate play more important roles in impacting treatment efficacy.

Keywords—Collective Antibiotic Tolerance (CAT), Beta-Lactam antibiotics, Intravenous drip (IV-drip) therapy, Extended Spectrum Beta Lactamase (ESBL), Beta-Lactamase production rate, optimize treatment

I. INTRODUCTION

Antibiotic resistance has become a significant global health concern due to the overuse and misuse of antibiotics, leading to the emergence of drug-resistant bacteria [1]. Among these bacteria, Extended-Spectrum-

Beta-Lactamase (ESBL) strains present particular challenges as they possess the ability to deactivate Beta-Lactam antibiotics [2]. As a result, optimizing treatment regimens becomes essential to improve treatment efficacy while minimizing the development of further resistance.

Previous studies have explored various approaches to combat antibiotic resistance, including the redesign of bacteriophages and bacteria, as well as the utilization of mathematical modeling [3, 4]. However, these approaches often come with limitations such as high costs and time consumption. Additionally, existing research on optimizing antibiotic treatments has focused on a limited range of parameters, primarily considering recovery time as a metric, and overlooking the long-term impact of multiple doses [5].

The aim of the current study is to address these research gaps by investigating the optimization of antibiotic treatments specifically for ESBL bacteria. A comprehensive approach was adopted that considers different types of intravenous drip pulse functions and develops a scoring matrix to evaluate treatment efficiency. By incorporating randomized regimens and analyzing population dynamics resulting from various pulse functions, the objective is to identify optimal ranges of treatment parameters for patients infected with ESBL bacteria. Crucially, the approach goes beyond a single-dose evaluation, encompassing the long-term effects of multiple doses administered over a defined interval of time.

The significance of the current research lies in providing a comprehensive framework for the optimization of antibiotic treatments. By considering factors such as time, resource consumption, and practicality of infusion, the aim is to evaluate treatment efficiency through multiple lenses. The findings will not only enable the customization of treatment regimens for ESBL bacteria but also hold potential applicability to other infected individuals. By addressing these research gaps and advancing the understanding of effective and personalized treatment strategies against antibiotic-resistant bacteria, this study contributes to the broader field of combating antibiotic resistance and improving patient outcomes.

Overall, this paper presents an investigation into the optimization of antibiotic treatments for ESBL bacteria, aiming to provide insights that go beyond conventional approaches and improve treatment strategies in the face of antibiotic resistance.

II. LITERATURE REVIEW

Ever since the discovery of penicillin in 1928, the antibiotic family commenced its upsurge in the therapeutic world, allowing human beings to overcome the fatality of bacterial infections for an extensive period [6, 7]. However, the rapid industrialization of drug production has promoted antibiotic accessibility while poverty and expensive healthcare have prevented financially disadvantaged patients from receiving adequate treatment in standard hospitals [8]. Such a dual effect has resulted in the overuse of drugs and the accelerated development of pathogenic tolerance [1]. The World Health Organization identifies antimicrobial resistance as one of the top ten global public health threats facing humanity [9]. According to a report published by the Centers for Disease Control and Prevention in 2019, more than 2.8 million antibiotic-resistant bacteria infections occur in the United States each year, leading to over 35,000 deaths [10]. Urgent action is required to alleviate the severity of this issue and suppress growing tolerance, salvaging time for substantial therapeutic advancements. Unfortunately, the diverse mechanisms employed by pathogens to develop resistance have posed significant challenges, hindering the discovery of a comprehensive solution [11]. Tolerance can derive from antibiotic inactivation, reduced membrane permeability, modification of target site, or transport pumps [12]. For instance, Extended-Spectrum-Beta-Lactamase (ESBL) bacteria, one of the most prevalent resistant strains, are resistant through antibiotic inactivation of Beta-Lactam antibiotics (Fig. 1). The bacterial species produce an inactivation molecule called Beta-Lactamase which alters the structure of the Beta-Lactam ring of the antibiotic, suspending its ability to inhibit cell-wall synthesis by binding to the Penicillin-Binding-Proteins (PBPs) [2].

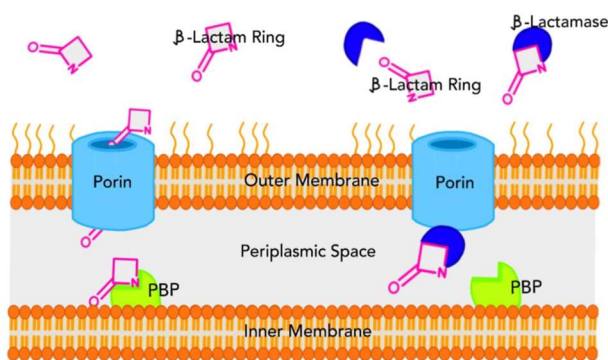


Fig. 1. Mechanisms towards resistance. The Beta-Lactam Ring of Beta-Lactam antibiotics lyse bacteria by inactivating penicillin-binding-proteins, which are essential to the construction of the bacterial cell wall. Beta-Lactamase produced by the bacteria can bind to the drug to inactivate it by altering its structure.

Due to the variety of resistant approaches, unfavorable and complex treatment responses frequently arise. Counterintuitively, a slower growth rate of the bacterial population might make it more difficult to suppress the infection due to the persistent effect. This effect occurs when the pathogen community slows down its growth rate during antibiotic treatment and reactivates its abilities and virulence as soon as the antibiotic effects lessen or disappear [13]. Furthermore, increasing the drug concentration often promotes bacterial recovery, a phenomenon known as the Eagle effect [14]. Thus, it is crucial to take into account the post-operative effect and the time interval between subsequent doses [15]. A recent study revealed that antibiotic treatment should follow the principle of “the shorter the better” [16]. These counterintuitive reactions underscore the importance of uncovering optimal ranges of parameters during antibiotic treatment. Blindly giving a treatment of antibiotics for as long as possible without considering optimal dosing strategies will exacerbate the infection.

Utilizing synthetic biology to control the timing and frequency of antibiotic dosing through periodic antibiotic dosing protocols is an optimal approach to suppress severity after infection and prevent further development of resistance. However, the discovery of new antibiotics has already substantially decelerated, resulting in an “innovation gap” [3]. Bacteria, on the other hand, continue to find new mechanisms to resist every developed lethal drug opponent. Other efforts to tackle this issue include redesigning bacteriophage, which could revolutionize and mutate with the bacteria as it goes [4]; redesigning bacteria itself by attempting to block the quorum sensing signal for Collective Antibiotic Tolerant (CAT) bacteria to attack the body; and achieve mutualism, etc. However, these approaches suffer from high costs and time consumption. Mathematical modeling and synthetic biology methods require comparatively less monetary investment and time and hold promise for identifying efficient treatments for tolerant infections.

A previous study on the optimization of antibiotic treatments proposed only recovery time as a metric for Intravenous-drip (IV) and continuous-injection antibiotic therapies [5]. However, there are situations where a singular metric will not be able to sustain. The effects of each dose of antibiotics act differently on the bacterial population, making it crucial to consider the long-term effect rather than solely the impact of a single dose. Furthermore, the definition of optimal treatment and characteristics affecting infusion have been overlooked. The study did not specify the optimal ranges of each parameter or define the most efficient treatment. When evaluating treatment efficiency, multiple factors such as time, expenditure, and net use of resources must be taken into account. Additionally, the study only utilized a single type of pulse function for modeling effects without considering other variations. It is crucial to consider the population dynamics until it becomes nearly impossible for the bacterial population to recover, which cannot be practically achieved with a single dose. A more comprehensive model is required that considers bacterial

dynamics throughout the entire treatment and evaluates efficiency through multiple lenses.

To resolve these problems, different types of IV-drip pulse functions were considered. A scoring matrix to evaluate the treatment efficiency was designed and used to assess randomized regimens to identify trends of each parameter (of the pulse function) for optimal treatments. The ESBL Bacteria dynamic model was used as the base model. However, instead of investigating only a single dose, the effects of multiple doses over a set interval of time were evaluated. The model was redesigned to demonstrate the population densities resulting from four different types of pulse functions (the Dirac delta, sine, normal distribution, and trapezoid functions) and created a scoring matrix to critique treatment practicality after randomization of five specific parameters (dosing period, dosing interval, locations of trapezoid turning points within a single dosing period (2 variables), and maximum rate of intravenous drip given). After using output data visualized through a radar chart and a box plot, the optimal ranges of antibiotic treatment regimens for the model patient were determined. The same equations can be utilized for any infected individuals to customize a treatment for ESBL bacteria. Further work focused on determining overall trends of the pulse function parameters for patients of different initial severity.

III. MATERIALS AND METHODS

A. Sample Model Utilizing Extended-Spectrum-Beta-Lactamase (ESBL) Bacteria

ESBL Bacteria are one of the most prevalent and extensively researched antibiotic-resistant bacterial species. Myriad experiments have been conducted to suppress the virulence of the strain and sufficient data have been obtained. Utilizing the dynamics and interactions of ESBL bacteria with Beta-Lactam antibiotics as a fundamental initial model is most favorable, as these interactions, the limits of antibiotic dosing, and the influencing pharmacodynamics and pharmacokinetics parameters, have all been profoundly experimented with. Sample data can be employed to construct pulse functions, resulting bacteria population decline, and sample score matrix models.

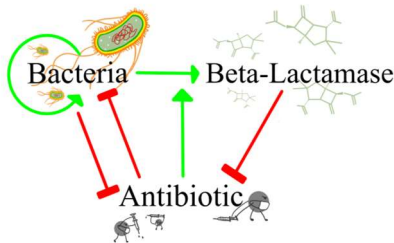


Fig. 2. Beta-Lactamase bacterial dynamics: The green arrow-headed line represents activation. The red bar-headed line represents inhibition. This graph models interactions between the bacterial population, beta-lactamase produced, and active antibiotics.

The bacteria population interacts with Beta-Lactamase and injected antibiotics in a complex dynamical system. Such dynamics can be utilized to analyze the effects of

different antibiotic treatments on the pathogen population through computational analysis. The final set of equations concerning the interaction between bacteria, beta-lactamase, and antibiotics will be generated based on the first-order and second-order activation and repression reaction rates present in the system. As Beta-Lactam antibiotics and ESBL are the most prevalent drug class and pathogen species, they have been extensively researched and thus provide a solid fundamental model to demonstrate different treatment effects.

B. Bacterial Dynamics and Ordinary Differential Equation (ODE) Models

The prototype ordinary differential equations came from a paper published by Meredith *et al.* [5]. The equations were adjusted to target IV-DRIP treatments. Bacterial interactions and dynamics allow the analysis of the change in population after each prolonged antibiotic infusion. By utilizing Ordinary Differential Equation (ODE) models and keeping all parameters except the IV-drip pulse function consistent, efficiencies of different types of IV-drip treatments can be determined. Reaction rates can be modeled depending on the activation or inhibition of each component in the interactive system, as demonstrated in Fig. 2. Rate and maximal constants as well as the Hill coefficient vary depending on the specific bacterial species, growth rate, and antibiotic class. A collective of three ordinary differential equations, five affiliate functions, and four base pulse functions (different variations of the IV-drip function) model the change in concentration of the bacterial population, beta-lactamase, and antibiotics. The four Intravenous-drip (IV-drip) pulse functions $k_{IV}(t)$ are Dirac-delta, sine, trapezoid, and normal distribution. Antibiotic treatments modeled in the pulse functions are infused within the same time intervals to ensure a fair comparison. Total antibiotic infused per period (and overall), or Area-Under-Curve (AUC), also remains constant.

Ordinary Differential Equations

$$\begin{cases} n' = (g - l)n \\ b'_{out} = lb_{in}^* - \gamma_2 b_{out} - [k_{IV}(t)]b_{out} \\ a' = v[k_{IV}(t)] - (b_{out} + \alpha b_{in}^*) \left(\frac{a}{1+a} \right) - \gamma_3 a - [k_{IV}(t)]a \end{cases} \quad (1)$$

Eq. (1): Prototype ordinary differential equations from Meredith *et al.* [5]. n' , b_{out} , a' are rate of change of bacterial population density, beta-lactamase concentration, and antibiotic concentration, respectively.

The rate of change of the bacterial population density (Eq. (1)) n' is dependent upon the growth rate (g) and lysis rate (l) of the current population (n). Growth rate g is expressed by $g = (1 - n) \left(\frac{\sigma_1}{\sigma_1 + a} \right)$. The equation consists of variables n , a (the current antibiotic concentration), and constant σ_1 (See Table I). Lysis rate l , with $l = \gamma_1 \left(\frac{a^H}{\sigma_2^H + a^H} \right) \left(\frac{\sigma_4}{\sigma_4 + b_{in}} \right)$, is a function of a , periplasmic Bla concentration per cell basis (b_{in}) (Equation: $b_{in} = \kappa \frac{r}{g + \gamma_4}$), the Hill Coefficient (H), and

constants γ_1 , σ_2 , and σ_4 (See Table I). The rate of change of antibiotic concentration a' (Eq. (1)) is modeled by $k_{IV}(t)$, b_{out} , b_{in}^* , a , and constants ν , γ_3 and α (Table I). Function bin consists of two crucial components κ and r . κ is a constant representing the efficiency of Bla ($\frac{k_{B_{in}} k_{B_{out}}}{\mu K_A}$) that correlates with bacteria growth rate (μ) (Table II). r is the activation rate of antibiotics ($\frac{a}{\sigma_3 + a}$). As demonstrated by Fig. 2 and the equations, directly increasing the antibiotic concentration will consequently increase the production of Beta-Lactamase. Therefore, irrational treatments maximizing antibiotic infusion are wasteful and potentially detrimental with opposing lethal effects on patients. Dynamics of bacteria support the importance of designing an optimal treatment not just for saving resources, but also to prevent lethal side effects.

C. Non-dimensionalized Parameters that Influence Treatment Efficiency and Key Assumptions

With this newly proposed treatment strategy, complex pre-treatment evaluations to investigate the bacterial population and its specific interactions with antibiotics are no longer necessary. Treatment can either be based on the typical models that are already determined or a customized version using personalized data through simpler tests. After non-dimensionalizing the equations, 14 variable parameter constants and 3 initial values are utilized in the model (Table I). Only 4, if necessary 5, are required to customize a treatment plan for individual patients (Table II). The source of each constant's prototype value is referenced in the "Definition" section of the table. The majority of the constant names and values came from the model proposed by Meredith *et al.* [5]. These 14 unit-less constants are dimensionalized ratios of pre-determined rate and half-maximal constants. The five essential parameters defined by patient status are bacterial growth rate (μ), initial bacterial concentration (N_0), initial antibiotic concentration (A_0), initial beta-lactamase concentration (B_0), and intracellular beta-lactamase production rate (k_{bin} (Table II)). Other constants are associated with the class of antibiotic used and predetermined. The Hill coefficient of 3 represents time-dependent antibiotics such as Beta-Lactam antibiotics [17].

Despite assumptions inherent within the equation, such that only the factors present in each Ordinary Differential Equation majorly impact the rate and population, this model also assumes that the rate of antibiotics infused intravenously is equivalent to the rate that antibiotic is pushed out. Additionally, the antibiotic is considered to possess only two major effects – inhibition of growth and promotion of lysis. Parameters γ_1 , γ_2 , γ_3 , and γ_4 are calculated with the ratio of a rate constant and μ (specific growth rate of the cell) and are altered in later case-by-case specific models. Parameter κ is a ratio of μ , k_{bin} (the production rate of intracellular Beta-lactamase), k_{bout} (the ejection rate of intracellular to extracellular Beta-lactamase), and K_A (the half-maximal constant of Bla degrading antibiotics) and therefore will also be modified

for later models. All other adjustable parameters are in the pulse functions of the IV-drip antibiotic treatment.

TABLE I. PARAMETERS IN PROTOTYPE ODE MODEL

Parameter Name	Definition	Typical Model Value
ν	Adjustment coefficient for intravenous antibiotic infusion.	0.5
α	Adjustment coefficient for level of protection provided by periplasmic versus extracellular Beta-lactamase [15].	0.01
β	Conversion factor from single cell to population [16].	0.001
H_1	Hill coefficient of antibiotic lysis rate [17].	3
κ	Beta-Lactamase Efficiency [18].	5.44E3
γ_1	Maximum lysis rate by general antibiotics [19].	62
γ_2	Maximum degradation rate of extracellular Beta-lactamase by antibiotics [20].	0.58
γ_3	Maximum degradation rate of extracellular Beta-lactam antibiotics [21].	0.51
γ_4	Maximum degradation rate of periplasmic Beta-lactam antibiotics [22].	0.25
σ_1	Half maximal constant for growth inhibition by general antibiotics associated with drug efficacy [18, 23].	0.24
σ_2	Half maximal constant for lysis by general antibiotics associated with drug efficacy [15].	1.29
σ_3	Half maximal constant for inducing Bla production associated with drug efficacy [24].	5.14
σ_4	Half maximal constant for periplasmic Bla protection associated with drug efficacy [15].	2.08E3

TABLE II. PARAMETERS BY PATIENT CONDITION

Parameter Name	Definition	Typical Model Value
μ	Bacterial growth rate [19].	0.8
N_0	Initial bacterial concentration [15].	0.1
k_{Bin}	Maximum rate of production of Beta-Lactamase [15].	0.1

D. Intravenous-Drip Pulse Function Modeling

Intravenous-Drip (infusion) therapy was chosen over injection due to several reasons. To begin with, other home-accessible antibiotic treatments, such as oral antibiotics, were not considered due to the infectiousness of ESBL bacteria, making it necessary for quarantine and hospitalization. Previous studies on beta-lactam antibiotic treatments for severe patients suggest administering continuous or prolonged infusions for critical care patients with septic shock, infected by bacteria with high MIC, suffering from lower respiratory tract infections, or suffering from infections due to non-fermenting Gram-negative bacilli to improve the clinical cure rate [25].

Considering the severity of infections by ESBL bacteria, a single dose of antibiotic injection will certainly not be enough even if that dose has an extremely high concentration, in which case lethal side effects will have occurred in the patient's body and additional beta-lactamase might have been produced as a defensive reaction. Doses of continuous infusion over an extensive

period produce longer recovery times and retained larger ranges of effective antibiotic concentration compared to injection [15]. Additionally, the IV-drip pulse functions take into account the short Post-Antibiotic Effect (PAE) of Beta-Lactamase bacteria by including a time interval between each prolonged infusion [16].

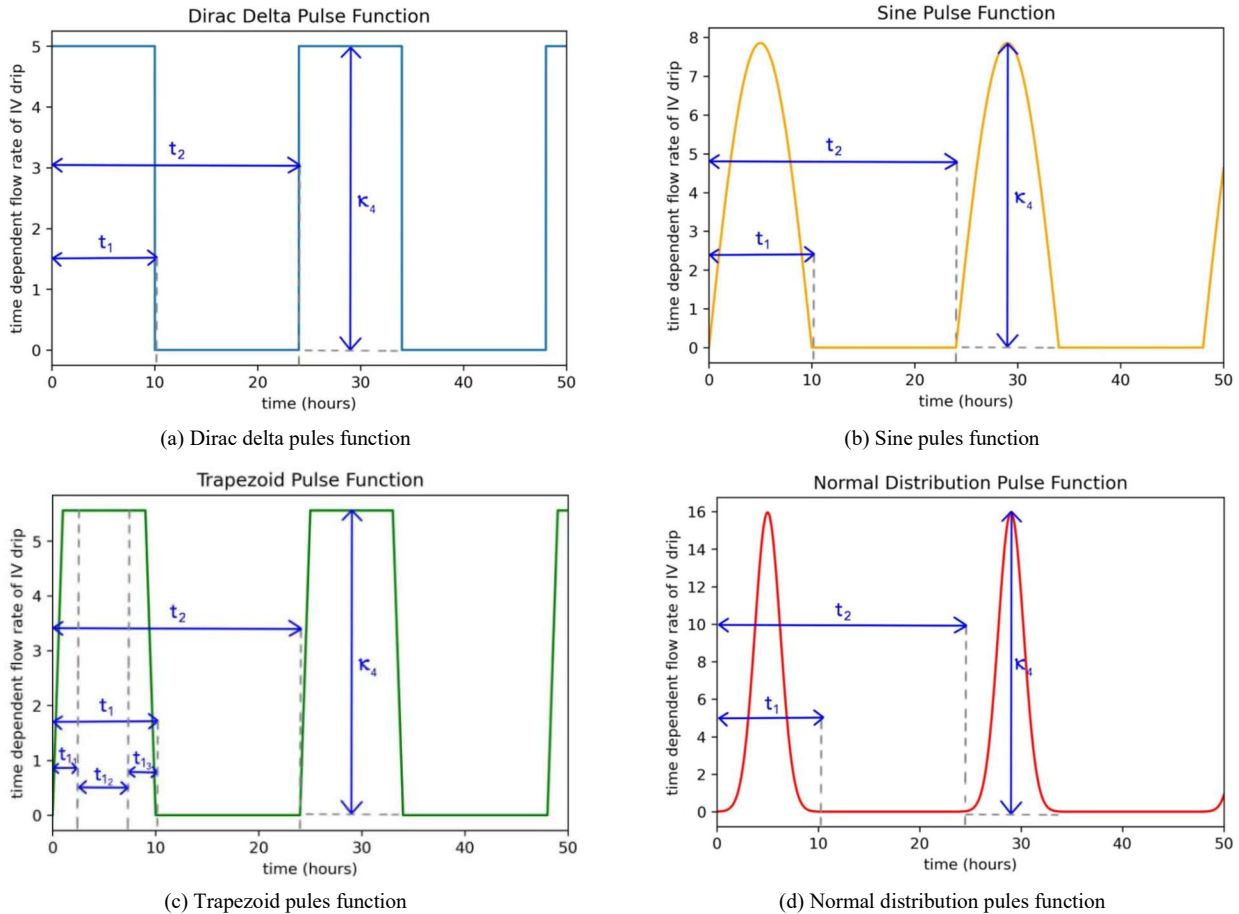


Fig. 3. Individual pulse functions. (a) The Dirac-delta pulse function. (b) The sine pulse function. (c) The trapezoid pulse function. t_{1_1} , t_{1_2} , and t_{1_3} are three variables unique to the trapezoid function, as marked by small blue arrows under the t_1 label. (d): The normal distribution pulse function. Parameters (t_1 , t_2 , and κ_4 for each function are labeled with blue arrows. These models show the rate of infusion during treatment within a time interval of 50 hours.

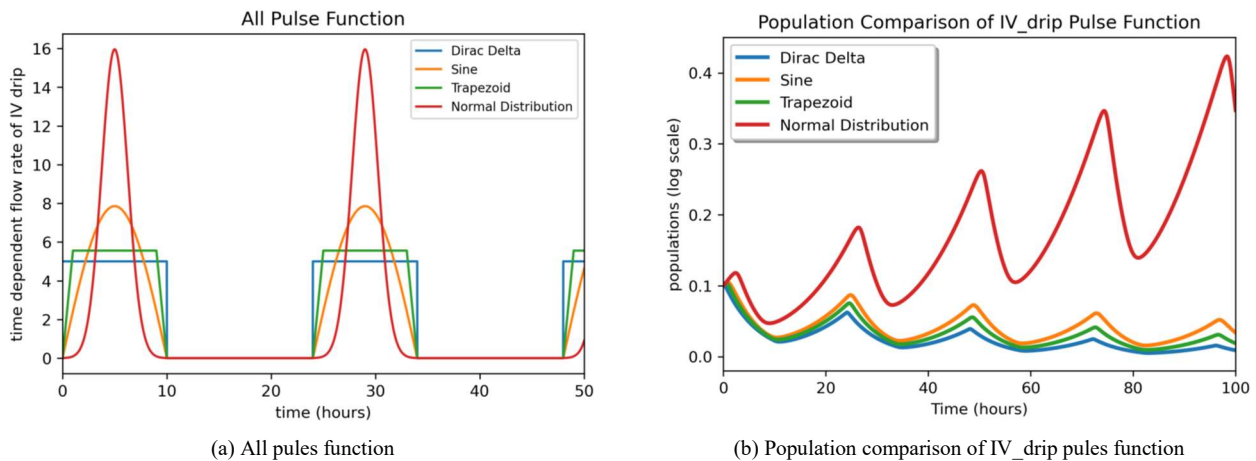


Fig. 4. All pulse functions and their correspondent treatment effects. (a) Model of the four pulse functions: Dirac-delta, sine, trapezoid, and normal distribution. Dosing interval, dosing period, and total antibiotic infused per period (Area Under Curve) were all kept constant. (b) Correspondent intravenous infusion treatment effects of the pulse functions: Dirac-Delta, sine, trapezoid, normal distribution.

The four most common infusion pulse functions – Dirac Delta, sine, trapezoid, and normal distribution were utilized to evaluate each corresponding treatment efficiency. The amount of antibiotic per infusion and complete treatment (Area under the Curve (AUC)), dosing period, and dosing interval are ensured to be the same to eliminate other potential reasons that might result in the corresponding bacterial population declination or increase. In Fig. 4(a), the Parameter t_2 (dosing interval) is set to 24 hours, corresponding to a daily period injection. The parameter t_1 is defined as the dosing period and set as 10 for the typical model. The maximum rate of infusion during Dirac-Delta treatment (κ_4) was set to 5 ($\mu\text{M}/\text{hour}$), the approximate mean of 0.5 and 10 (a range considered middle-low antibiotic concentration). 0.5 $\mu\text{M}/\text{hour}$ is the mark where antibiotic concentration becomes high enough to cause minimal cell lysis while 10 $\mu\text{M}/\text{hour}$ becomes relatively high a rate, to the extent where one dose might be able to eradicate the bacterial population at the site of infection and lead to infinite recovery time [21]. By more than 10 $\mu\text{M}/\text{hour}$, side effects will have occurred in the human body. Therefore, κ_4 for the typical model is set as 5 $\mu\text{M}/\text{hour}$. κ_4 for all other functions – sine, trapezoid, normal distribution – are adjusted as the maximum rate throughout the treatment to have an equivalent AUC (area under the curve). The trapezoid and normal distribution functions have a few other unique variables, as labeled in Figs. 3(c) and 3(d). In the trapezoid function, parameters t_{1_1} , t_{1_2} , and t_{1_3} represent time intervals when the rate of injection is increasing, constant, and decreasing, respectively.

E. Optimal Type of Pulse Function and Relevance

Results from modeling of the bacterial population after treatment within 100 hours of four doses revealed that the Dirac-Delta, trapezoid, and sine functions are similarly efficient while the normal distribution pulse function treatment caused the bacteria population to experience a net increase in population. Out of the other three, the Dirac-delta and trapezoid are more competent. The fact that the normal distribution treatment caused reversed effects in treatment further emphasizes the importance of finding the optimal pulse function for treatment. An inefficient pulse, despite having the same amount of total antibiotics delivered, will potentially have fatal consequences. The normal distribution function's extended period of low-rate treatment was likely ineffective in lysing the bacteria. After reaching a low point after each treatment, due to exposure to antibiotics, the bacterial population further increased its mechanism to resistance and rapidly expanded in population. Thus, the rate of infusion during treatment is crucial to consider. From the modeling results in Fig. 4(b), the Dirac-Delta and the trapezoid function are the most efficient and closest together. Because the Dirac-Delta is a special variation of the trapezoid function – when t_{1_1} and t_{1_3} are zero – and that the trapezoid function is more flexible to adjust for randomization due to a larger number of parameters, the treatment efficiency of different

randomized trapezoid pulse function IV-drip treatment regimens will be assessed.

F. Definition of the Score Matrix and Models

The score matrix is defined by five parameters correlating with variables obtained by data randomization: time period, time interval, maximum rate of the intravenous drip given, total drug (area under the curve), and total treatment number (Fig. 5). It is crucial to consider other contributing factors to an optimal treatment despite the fastest recovery time. The time interval and time period of intravenous drip delivered each account for 15% of the final score. The total drug delivered (AUC) accounts for 25%, and the total treatment number accounts for 35%. κ_4 , or the maximum rate of injection during the treatment period, accounts for the 10% remaining portion. The worth of each score parameter is determined through research on their impacts on the final result of treatment and the least amount of resources used. An optimal treatment consists of the least amount of total antibiotics and the shortest treatment time in preventing side effects and reducing wasted resources. The total amount of antibiotics is affected by κ_4 (the maximum rate of antibiotic infusion during treatment) and the total drug. Both of these variables are optimally minimized. Total drug (25%) accounts for 15% more than κ_4 (10%) as it is common sense to consider the total over each separate dose. Total drug (25%) and total treatment number (35%) account for a difference of 10% since although it is optimal to use as few drugs as possible, the number of hours/days the patient would need to stay in the hospital would compose the main portion of expenses in treatment. A recent study reveals that total ICU costs comprise 38.51% drug costs and 24.45% medical tools and equipment [26]. The total expenditure of IV-antibiotic treatment is constituted by a multitude of factors and not only the costs of the drugs. Given that the patients are infected with superbugs, it would be most appropriate for quarantine and careful administration in the hospital. Thus, it is important to also take into account to a substantial degree the time expended by medical and nursing staff, charge of disposable materials and overhead, and the general cost of hospital stays. Thus, the total treatment number or total treatment time amounts the most in the score matrix. The remaining 30% is equally shared between the time period (15%) and time interval (15%) of each dose. As stated, given the patient's condition of severe infection of CAT bacteria, the treatment will most likely be conducted in a hospitalized condition to prevent the spread and further resistance of the species. The time interval and time period of each dose are of similar importance. They both contribute to the total time a patient has to stay hospitalized.

From the results of Fig. 4(b), the Dirac-delta pulse function treatment appears most competent, along with sine and trapezoid close to its lead in efficacy. As the Dirac-delta is a special variation of the trapezoid function, it was established to manipulate the parameters of the trapezoid function to optimize treatment. Parameters t_1 ,

t_{1_1} , t_{1_2} , t_{1_2} , t_2 , and κ_4 , as illustrated in Fig. 3(c), were randomized 20000 times to return a list of scores and their correspondent variables. Ranges of each parameter were limited with maximum and minimum values. The maximum values of κ_4 , t_1 (dosing period), t_2 (dosing interval), treatment number, and total drug (Area Under Curve AUC) were set to 10, 10, 24, 50, and 5000 ($\kappa_{4max} * t_{1max} * \text{treatment number}$), respectively. The limit of values t_{1_1} , t_{1_2} , and t_{1_2} were determined by the current randomized t_1 value. This ratio was determined due to previous research that revealed for Beta-Lactam antibiotic treatments, which are time rather than concentration-dependent, when the $T > MIC$ (time above minimal inhibitory concentration) is between 40%–50%, the patient survival rate is approximately 90%–100% [27]. Whereas when $T > MIC$ is less than 20%, the mortality rate was virtually 100%. A $T > MIC$ much greater than 40%–50% will also result in potentially negative effects due to the induction of Beta-Lactamase and side effects on the human body. The time it takes to reach a successful and completed treatment is the time within the set time interval of 3000 when the bacterial population density reaches the predefined threshold of $1e-10$. These limit values do not have a specific research-based definition but are rather set as general boundaries. The model is simplified and the actual optimal range will be determined after modeling and analysis of trends of the returned score matrix. To display the final result, a radar chart, and a box plot are utilized to present the score and the optimal parameters obtained from randomization. Colors on the radar chart exhibit the score obtained and each axis represents one parameter. The ‘jet’ colormap of matplotlib was used to clearly visualize the difference in scores. Two charts of complementary colors (red and blue) were produced to demonstrate the trend in the difference of parameters between high and low scores. The box plot is utilized to present the optimal range of parameters to doctors and patients in the most straightforward manner possible. The box plot only consists of high-scoring scores.

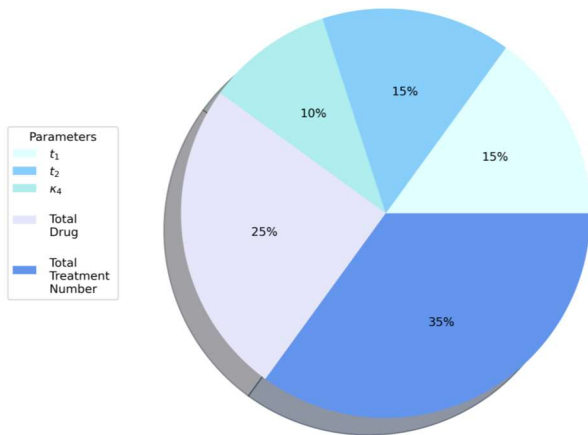


Fig. 5. Score matrix parameter importance distribution pie chart: Parameter t_1 determines 15% of the final score of each treatment. Parameter t_2 determines 15% of the final score of each treatment. Parameter κ_4 determines 10% of the final score of each treatment. The total antibiotic amount determines 25% of the final score of each treatment. The total treatment number determines 35% of the final score of each treatment.

G. Beta-Lactamase Dynamic Model Practicality (Case by Case)

After the creation of a typical model, more specific models for patients with different infection conditions were made. In these additional models, patients are categorized into mild and severe infections. As presented in Table II, the typical model’s growth rate of bacteria (g), the initial population density of bacteria (N_0), and the rate of production of beta-lactamase (k_{Bin}) were set to 0.8, 0.1, and 0.1, respectively (Table II). These are the critical variables to modify when considering patients with different degrees of sickness. Table III presents altered values and ranges for case-by-case infections (Table III). Patients with a mild infection were set to have g in range (0.1, 0.8), N_0 in range (0.01, 0.1), and a k_{Bin} of 0.1. Severely infected patients have a g in range (0.8, 4), N_0 in range (0.1, 1), and a k_{Bin} of 0.1. The k_{Bin} of these two models were not changed because this specific parameter is difficult, therefore, only when patients demand a highly specific treatment shall this be altered. Such particularly specific treatments can be appropriate for severely infected patients. So, despite the typical model for severely infected patients, treatments that target different Beta-Lactamase production rates are further optimized. In the two different models, k_{Bin} were separately set to a range of (0.01, 0.1) and (0.1, 1) for slow and rapid production rates, respectively. Initial beta-lactamase concentrations and antibiotic concentrations were kept the same throughout to control and minimize changes in variables. Randomization of each parameter within the designated range was completed for a total of 20000 times for each model. Similar methods were used from the most typical model but extra axes were added to the produced radar charts to demonstrate the changed variables in their corresponding ranges. Box plots were also produced to specific optimal values.

TABLE III. ALTERED PARAMETERS FOR CASE-BY-CASE SCENARIOS

Parameter	Mild Typical k_{Bin}	Severe Typical k_{Bin}	Severe High k_{Bin}	Severe Low k_{Bin}
μ	(0.1, 0.8)	(0.8, 4)	(0.8, 4)	(0.8, 4)
N_0	(0.01, 0.1)	(0.1, 1)	(0.1, 1)	(0.1, 1)
k_{Bin}	0.1	0.1	(0.01, 0.1)	(0.1, 1)

IV. RESULTS

A. Optimal Range of Essential Parameters for Typical Patients

By randomizing parameters of the trapezoid pulse function 20000 times, scores and constant records of successful trials were returned. Three radar charts (Fig. 6) and a box plot (Fig. 7) were generated to demonstrate the final optimization result. All treatments, treatments scoring lower than 2.5% of all scores, and treatments scoring higher than 97.5% of all scores were individually plotted onto the three separate radar charts (Fig. 6). Adjustments in color-score representation were done to better visualize the results. Color differences were

amplified in low and high-scoring charts, with a scale from contrasting colors blue and red in the ‘jet’ colormap used.

Color represents score – blue-scheme lines have lower scores than red-scheme lines, with dark blue being the lowest score that successfully suppressed the bacterial population to the low limit and dark red scores being the highest and most efficient. In Fig. 6(a), the overwhelming majority of lines are green, since they are close to the median (50%) score. Comparing each axis on the high

and low score radar charts will present a trend in each parameter that results in the most effective treatment for the typical patient. In Fig. 6(c), within the dosing period (t_1), it is optimal to maximize t_{1_2} and minimize the other two (t_{1_1} and t_{1_3}). Counter-intuitively, maximizing the rate of infusion (κ_4) will not result in the highest scores. The empty triangular area reveals a minimum limit in t_2 and κ_4 – treatments given under the specific time interval and κ_4 limit will lead to inefficiency.

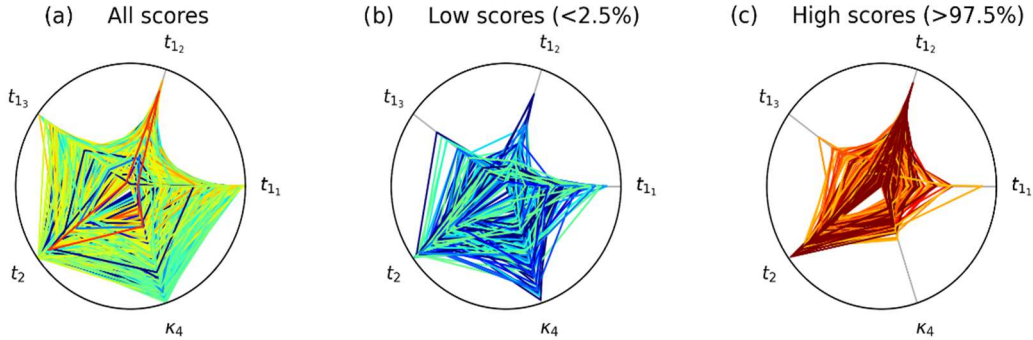


Fig. 6. Radar charts: Representation of the score matrix reproduced from 20000 randomized data sets, only showing data that successfully reached the population low limit before the predetermined maximum time. (a) Regimen of all returned scores. Blue are lowest scores, red are highest scores, green are median scores. (b) Regimen of returned scores that are lower than 97.5% of all scores (bottom 2.5%). (c) Regimen of returned scores that are high than 97.5% of all scores (top 2.5%).

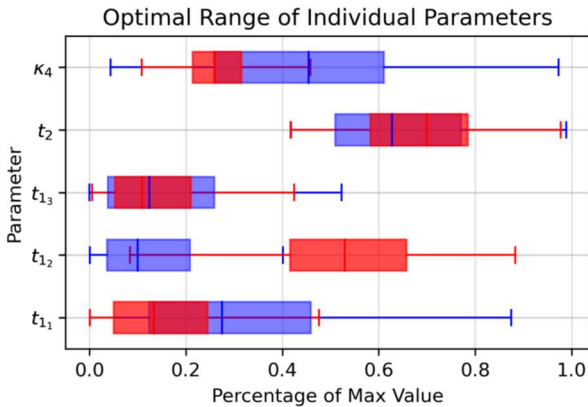


Fig. 7. Original model box plot: The box plot presents the range of each parameter as a ratio with their predefined maximum values.

To further specify the highest scoring parameters for practical use by doctors and patients, a box plot was created to better present the ranges of desirable parameters. This visual representation only shows data from Figs. 6(b) and 6(c). The box plot scales optimal values to a percentage ratio with their pre-determined maximum values. It is suggested for doctors and patients to select within the box range specifically for the high scores while avoiding the low scores – in particular for

parameters that present abundantly different ranges between the two types of scores.

B. Optimal Range of Essential Parameters for Patients of Different Degree of Infection

Similar techniques were utilized for patients under different infection conditions. However, more axes were added to the radar charts to show the randomization and scale change in the altered conditions – growth rate μ , initial bacterial population density N_0 , and Beta-Lactamase production rate k_{Bin} (Fig. 8). The distinct shapes and empty areas in the center disclose the essential limits and boundaries of each parameter. As the typical original model, most lines in the ‘All score’ radar chart are colored in green, meaning they fall within a range very close to the median (Q2 or 50%) score.

Box plots are additionally created. Similar general trends can be found in treatment ratios despite the varying growth rate, initial population density, and Beta-Lactamase production rate. The maximum values or limits for each parameter are controlled throughout the modeling process. The doctor and/or patient can utilize the boxes to look at the general ratio trend in the box plot for designing an appropriate treatment regimen.

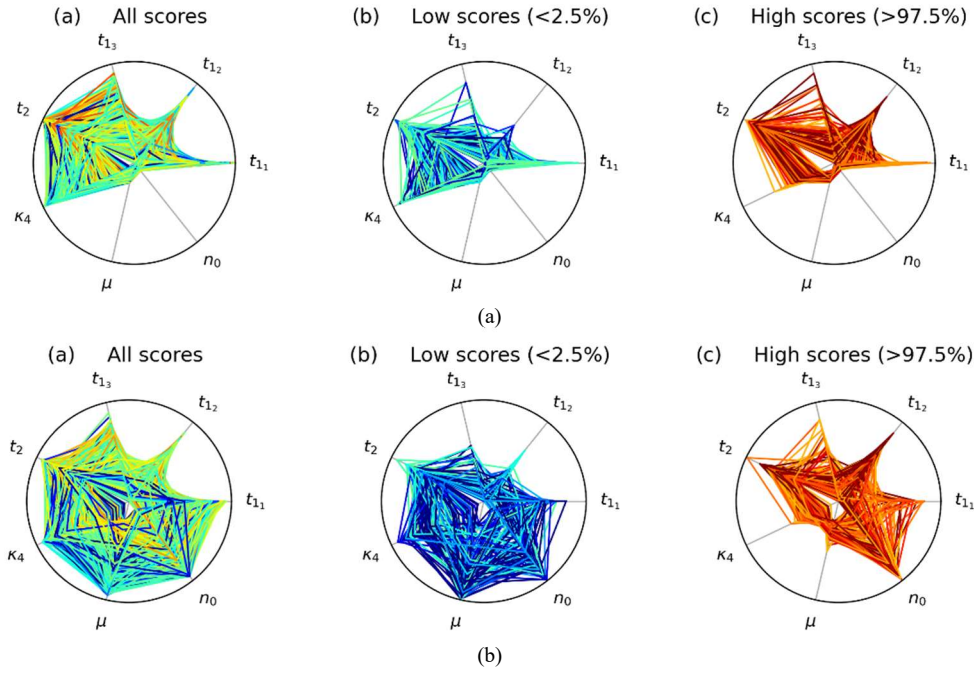


Fig. 8. Score matrix radar chart representing different degree of severity. Data randomized within a range of predefined growth rate and initial bacterial population density. (a) Mildly Infected Patients with Typical $k_{B,In}$. Regimen of all scores, low scores, and high scores for patients with a growth rate within range (0.1, 0.8) and an initial population within range (0.01, 0.1). (b) Severely Infected Patients with Typical $k_{B,In}$. Regimen of all scores, low scores, and high scores for patients with a growth rate within range (0.8, 4) and an initial population within range (0.1, 1).

V. DISCUSSION

A. Appropriate Ranges of Parameters for Individual Patients Infected with ESBL Bacteria

1) Typical patient

From data returned from the typical patient, one can observe multiple trends when comparing the low with high score charts (Fig. 6) as well as when analyzing the box plot (Fig. 7).

a) Counter-intuitively κ_4 possesses a limit value in the high-scoring data below the predetermined limit

This further reinstates Beta-Lactam antibiotics' time but not concentration-dependent property [26]. According to the report by Craig, the concentration will reach a certain point, four to five times higher than the MIC (minimal inhibitory concentration), where further increase will no longer render the treatment more efficient. This is suggested by the distinct angle limit of κ_4 on the returned radar chart. Further increase in it will result in a similar speed of treatment but much higher costs and demand for resources. The box plot further reinstates this trend. In the box plot, the optimal κ_4 values are very densely distributed within a small range, from around 20% to 30% of its maximum value. It is recommended for the treatment to consist of κ_4 within this range, instead of giving as high a dose as possible.

b) It is optimal to maximize the ratio between t_{12} – the time when the rate of infusion reaches the maximum (top edge of the trapezoid) – and t_{11} or t_{13}

It is not just about having t_{12} maximized, it is also important to scale the ratios of it with the other two values. This is because of the Beta-Lactam antibiotic's time-dependent property, as for this class of anti-

microbial drugs, it is most important to consider the time of infusion and the concentration per time period. This can be demonstrated by how the Dirac-Delta (special trapezoid) pulse function treatment was more efficient than the original predefined trapezoid function (Fig. 4(b)). The Dirac-delta was most efficient in treating the typical patient with controlled model time and concentration values with both its t_{11} and t_{13} values being zero. However, direct utilization of the Dirac-Delta function is proved impractical by the randomized data because even though t_{12} seems optimally maximized (as ratios with t_{11} and t_{13} , none of the majority of treatment regimens with high scores actually had a t_{12} that reached its absolute maximum t_1 . It was mostly within the 60%–80% (0.6–0.8) ratio range. Both high and low scores had extremities that reached 100%, revealing the lack of correlation between a maximized t_{12} and efficient treatment. What is most important to consider is the ratio difference between the three trapezoid parameters t_{11} , t_{12} , and t_{13} , instead of inconsiderate maximization of the parameter with the highest infusion rate (as is with the Dirac-Delta function).

c) Incessant and rapid dosing with short intervals do not increase treatment efficiency

There is a relative minimum that t_2 must reach in order to constitute an efficient treatment. The radar chart and box plot further reveal the limit of the parameter t_2 (time interval between succeeding treatments). One thing to note is that despite the low scores being not optimal, they still represent treatment that in the least was able to cure the infection till the population low limit ($1e-10$) (Table II) within the time limit. Both boxes, blue or red, in this case, presented a minimal limit at around 50% to 80% of t_2 's maximum value. Another thing to keep in mind is

that both scores' bar ends were around the value 0.42 because the t_2 values were generated purposefully to stay above the predetermined $t_{1\max}$ value of 10. The ratio of 10 and $t_{2\max}$ value 24 is approximately 0.42 or 42%.

d) *The high-scoring radar chart demonstrates a strong correlation between parameters t_2 and κ_4*

This is something that cannot be observed through the box plot. The empty triangular area reveals that having low-concentration doses for a short dosing interval, even if infused for a long dosing period, will not be optimal. Furthermore, the darkest red (highest scores) correlates with high t_2 and high κ_4 .

e) *There is a huge distinction in parameter t_{1_2} in high versus low scoring regimens*

The blue box of the low scores ranges from around 5% to 20% of the maximum value while the red box of high scores ranges from around 40% to 65%. This presents a strong correlation in efficiency of treatment concerning of value of parameter t_{1_2} . This is an important value to carefully consider when designing treatment regimens.

f) *The t_{1_3} value for high scores is completely contained within the range for low scores, revealing its lack of specificity compared to other parameters*

This makes sense because t_{1_3} represents the period of time after the rate of infusion sustains at its maximum. It is highly likely that the treatment is already efficient enough before the start of this period, rendering its precise values not as important. However, it is still clear that an optimal treatment would consist of a lower t_{1_3} so most infusion time would be dedicated to maximum rate of infusion t_{1_2} .

2) *Mild or severely infected patients without the knowledge of Beta-Lactamase production rate*

Radar charts for mild or severely infected patients with typical k_{Bin} (Beta-Lactamase production rate) consisted of additional axes presenting their μ (growth rate) and n_0 (initial bacterial population). As shown, μ and n_0 of the mildly infected patient stayed within a minimized range between 0.1–0.8 and 0.01–0.1, respectively (Fig. 9(a)). On the other hand, μ and n_0 of severely infected patient were within the range 0.8–4 and 0.1–1. The box plots additionally demonstrate low and high scoring parameters' correlations and general trends in a clearer fashion.

a) *All highest-scoring treatment regimens consist of minimal μ close to 0.8 and a widely distributed n_0 ranging from 0.1 to 1, as demonstrated by the radar chart*

This reveals the significance of the growth rate as compared to the initial condition. A higher growth rate will cause the bacteria to have stronger defense mechanisms against the antibiotic and recover from its suppressing effects quicker. The initial bacterial population density does not seem to matter as much because superbugs are not hard to treat because they produce a large-scale infection, it is because they can resist, retrieve, and even increase in population due to their defense mechanism after treatment of antibiotics. The μ for mild infections alter within a smaller range and is considered low anyways, therefore its distribution is not as clear as that of severe infections.

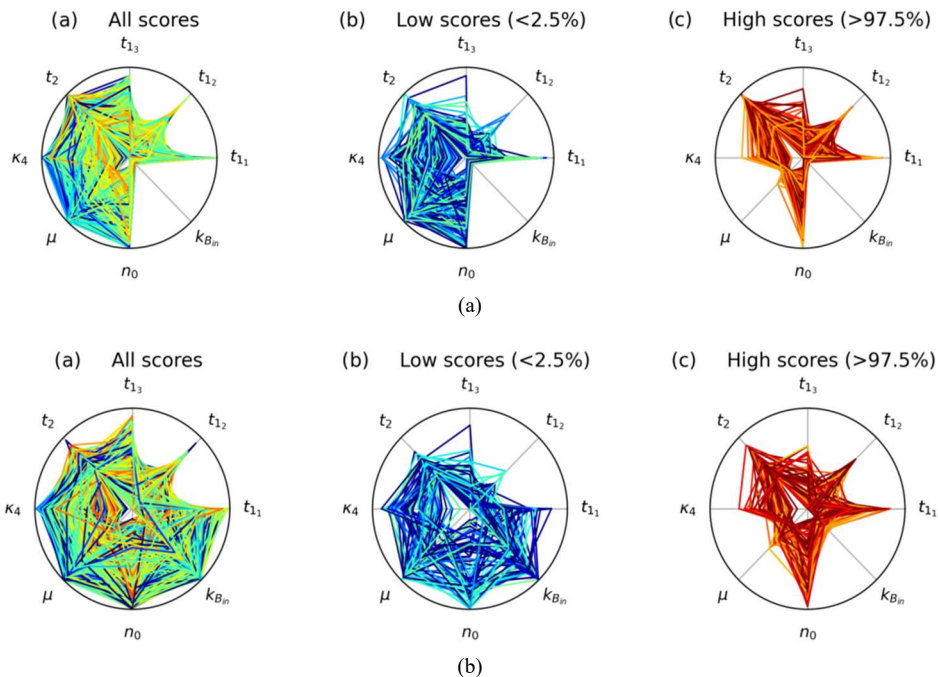


Fig. 9. Score matrix radar chart representing different degree of severity with altered Bla production rate. These two sample score matrix-critiqued treatments took a step further in specific treatment and additionally altered k_{Bin} , presented on the radar charts with an additional axis. (a) Severely infected patients with low. Present treatment regimen for patients with severe-ranged growth rate and initial population density as well as within range (0.01, 0.1). (b) Severely infected patients with high same as Fig. 9(a) except an altered k_{Bin} within range (0.1, 1).

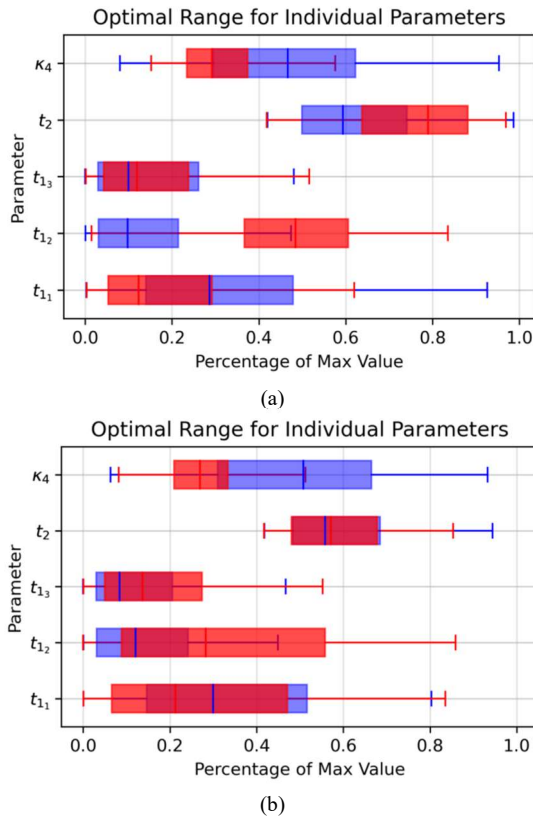


Fig. 10. Score matrix box plot representing different degree of severity. (a) Box plot of patients with mild growth rate and initial density. μ and N_0 within ranges (0.01, 0.1) and (0.1, 0.8), respectively. $k_{B_{in}}$ set as 0.1. Box plot consists of high and low scoring boxes for mildly infected patients, showing each treatment parameter range. (b) Box plot of patients with severe growth rate and initial density. μ and N_0 within ranges (0.1, 1) and (0.8, 4), respectively. $k_{B_{in}}$ set as 0.1. Box plot consists of high and low scoring boxes for severely infected patients.

b) *Low and high scoring t_{1_1} for mild and severe infections consist of a larger overlap compared to the original*

This makes sense because, in both situations here, the growth rate and initial population density are also altered each time, providing a larger variety of conditions and therefore a larger different range of treatments. Nevertheless, both stayed within a very similar range. Note that despite low-scoring parameters being unfavorable, they still present treatment regimens that successfully treated the patient within the predetermined time limit. As shown, neither low nor high scores genuinely passed 50%. Thus, it can be further concluded that it is important to keep t_{1_1} under a relatively minimized condition. The larger variability that the severe box has compared to the mild box is reasonable due to its larger net variability in growth rate and initial condition. Mild infections' μ and n_0 falls within ranges (0.1, 0.8) and (0.01, 0.1) with net differences of 0.7 and 0.09, respectively. While those with severe infection fall within ranges (0.8, 4) and (0.1, 1) with net differences of 3.2 and 0.9.

c) *For mild patients, the parameter t_{1_2} demonstrates a similar optimization trend with the*

original such that it remains significantly longer than parameters t_{1_1} and t_{1_3}

For severe patients, the wider range is due to the variability of growth rate and initial condition. The mild box plot (Fig. 10(a)) shows a much clearer pattern that resembles the original (Fig. 7). The higher growth rate for severe patients will result in stronger resistance and greater comeback when infused with high concentrations of antibiotics for a longer period of time. Therefore, as shown in Figs. 7(b) and 10(b), it is occasionally optimal for t_{1_1} or t_{1_3} to be equal or higher than t_{1_2} to prevent further induction of growth rate and Beta-Lactamase.

d) *As with the typical model, it is optimal for t_2 to be higher than its limit*

However, a clear difference is revealed when comparing the high-scoring t_2 ranges for mild and severe infections. For mild infections, with lower growth rate and initial population, the optimal time interval is evidently higher than that of severe infections. This makes sense because a less frequent dosing is more favorable when treating infections with a slower growth rate because frequent dosing will potentially induce further resistance and be more costly yet inefficient.

e) *The optimal ranges of κ_4 for both mild and severe infections are distributed similarly with the original, revealing its strong correlations and steady trend for efficient treatment despite differences in condition*

It is evident that κ_4 optimally falls within the range (0.2, 0.4) for all cases. The low-scoring parameters are also generally distributed within the same ranges. These results strongly suggest doctors to design treatments with a maximum rate of infusion at around 2–4 (with the predetermined maximum value of 10).

B. Severely Infected Patients with High or Low Beta-Lactamase Production Rate

Severely infected patients are further divided into groups of high Beta-Lactamase production rate and low Beta-Lactamase production rates due to their difficulty to cure and the necessity for even more specific treatments. A $k_{B_{in}}$ axis is added to show the difference in production rate of Beta-Lactamase between the two produced charts (Figs. 9(a) and 9(b)). The general trend for the two in the box plot is extremely similar, revealing that all severe infections, despite the Beta-Lactamase production rate, can be treated with similar regimens.

1) *Most patterns and trends for both cases resemble those of severely infected patients with predetermined typical $k_{B_{in}}$*

The only differences are that the general distribution of t_{1_3} for both are higher than t_{1_2} , and that the optimal t_2 differs significantly from the original and mild infection models. The box plots (Fig. 11) look highly identical to that of normal severe infections except that t_{1_3} are now the highest general value. For these two cases, the third part of trapezoid infusion should be carefully considered unlike mild and the original situations.

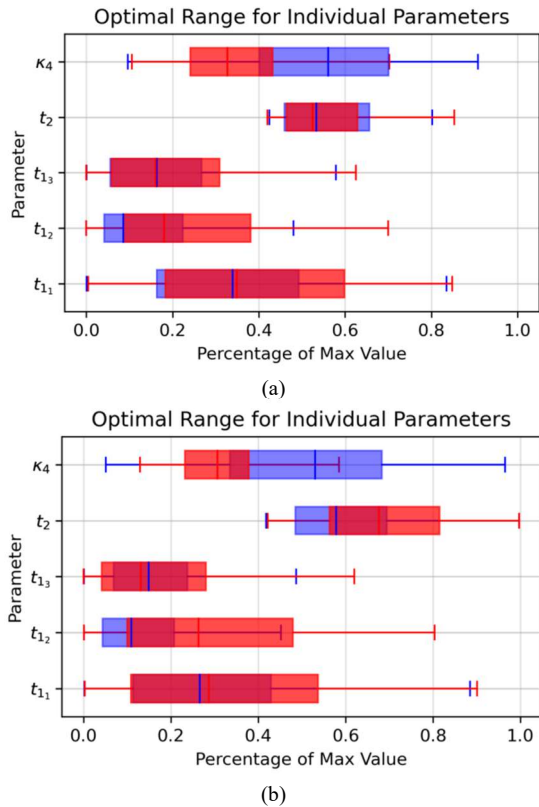


Fig. 11. Score matrix box plot representing severely infected patients with different k_{in} , μ and N_0 ranges are kept constant with typical severely infected patients (Fig. 10(b)). (a) Severely Infected Patients with Low k_{Bin} . Box plot presenting high and low scoring ranges of severe infections with low Bla production rate. (b) Severely Infected Patients with High k_{Bin} . Box plot presenting high and low scoring ranges of severe infections with high Bla production rate.

2) The radar charts reveal a strong correlation between k_{Bin} and treatment efficiency. However, the box plot did not vary much from the severe infection model with typical k_{Bin}

Nevertheless, a low k_{Bin} will render the treatment more effective. This makes intuitive sense because the slower the Beta-Lactamase production rate, the fewer antibiotics will be inactivated, and the more lysing of bacteria. To sum up, changes in k_{Bin} and g are much more determinant to the treatment efficacy than changes in n_0 .

3) A slower Beta-Lactamase production rate will require a longer time interval t_2 and a more rapid will require the subsequent doses to be more frequent

However, it is important to note that the dose should still not be too frequent because it will be easy to induce side effects and further resistance.

4) κ_4 remain at identical ranges

This reveals the significance of this parameter to always sustain within a certain range instead of infusing maximum drugs to the patient.

VI. CONCLUSION

Modeling of treatment effects of the four pulse functions on a model strain of ESBL bacteria revealed the importance of choosing an appropriate pulse function and

designing optimal pulse function regimens for antibiotic-resistant bacterial infections. If designed improperly, the infection will exacerbate and potentially be lethal for the patient. Out of the four pulse functions, the Dirac-delta, or the special trapezoid function was the most efficient. Thus, parameters of the trapezoid function were manipulated and randomized to uncover the optimal ranges of each variable. A score matrix was produced to critique the treatment's efficiency and practicality. Radar charts and a box plot were returned after randomization and judgment by the score matrix for the convenience of doctors and patients. Results further demonstrated Beta-Lactam antibiotic's time but not concentration-dependent characteristics. More specific patient conditions with varying growth rates, initial bacterial population density, and Beta-Lactamase production rate were modeled with the same methods using the same population of ESBL bacteria and identical limits. Trends were generally analogous. Results were akin to the typical model. κ_4 was most constant, and despite the condition, it remains within a general range of 3–6. t_2 is generally remained above the 50% mark, or the specific value of 12. Out of the other three parameters, most of the time is it optimal for t_{1_2} to be the longest during the time period. However, t_{1_1} is generally longest in optimal treatment regimen for patients with low or high (especially high) Beta-Lactamase production rate.

In the future, efforts can be taken to improve the practicality of the score matrix and the limits of each parameter. Furthermore, a library could be formed with more mechanisms of antibiotic resistance to target a broader scope of patients. Hopes are that patients will be able to walk into a clinic and get tested minimally for the main infection population resistance mechanism, bacterial growth rate, and initial population density, and return to an optimal treatment regimen with ranges of each parameter, which they can adjust for personal preferences or grant the doctor to directly utilize the highest scoring treatment plan. However, it is important to note that mathematics models are often simplified scenarios of infection. Instantaneous monitoring of patients is necessary during treatment and accurate values must be returned from hospital tests before utilizing these models for design.

CONFLICT OF INTEREST

The authors declare no conflict of interest.

AUTHOR CONTRIBUTIONS

Irene Yicheng Jiang and Will Cao conceived and planned the research. Irene Yicheng Jiang conducted the research, analysed the data, performed the calculations, drafted the manuscript, and designed the figures. Will Cao discussed the results and commented on the manuscript. All authors had approved the final version.

ACKNOWLEDGMENT

We would like to thank Meredith *et al.* [15] for the prototype model and sample data.

REFERENCES

- [1] R. Laxminarayan, "The overlooked pandemic of antimicrobial resistance," *The Lancet*, vol. 399, 10325, pp. 606–607, 2022.
- [2] T. Naas, S. Oueslati, R. A. Bonnin, *et al.*, "Beta-Lactamase Database (BLDB) – structure and function," *Journal of Enzyme Inhibition and Medicinal Chemistry*, vol. 32, no. 1, pp. 917–919, 2017.
- [3] L. Gao, H. Wang, B. Zheng, *et al.*, "Combating antibiotic resistance: Current strategies for the discovery of novel antibacterial materials based on macrocycle supramolecular chemistry," *Giant*, vol. 7, 100066, 2021.
- [4] D. M. Lin, B. Koskella, and H. C. Lin, "Phage therapy: An alternative to antibiotics in the age of multi-drug resistance," *World Journal of Gastrointestinal Pharmacology and Therapeutics*, vol. 8, no. 3, p. 162, 2017.
- [5] H. R. Meredith, A. J. Lopatkin, D. J. Anderson, and L. You, "Bacterial temporal dynamics enable optimal design of antibiotic treatment," *PLoS Computational Biology*, vol. 11, no. 4, e1004201, 2015.
- [6] L. Kim, "The science of antibiotic discovery," *Cell*, vol. 181, no. 1, pp. 29–45, 2020.
- [7] C. Ardal, M. Balasegaram, R. Laxminarayan, *et al.*, "Antibiotic development—economic, regulatory and societal challenges," *Nature Reviews Microbiology*, vol. 18, no. 5, pp. 267–274, 2020.
- [8] B. Li and T. J. Webster, "Bacteria antibiotic resistance: New challenges and opportunities for implant-associated orthopedic infections," *Journal of Orthopaedic Research*, vol. 36, no. 1, pp. 22–32, 2018.
- [9] World Health Organization, "Global antimicrobial resistance and use surveillance system (GLASS) report," 2021.
- [10] *Antibiotic Resistance Threats in the United States, 2019*, US Department of Health and Human Services, Centres for Disease Control and Prevention, 2019.
- [11] J. Dugassa and N. Shukuri, "Review on antibiotic resistance and its mechanism of development," *Journal of Health, Medicine and Nursing*, vol. 1, no. 3, pp. 1–17, 2017.
- [12] A. J. Lopatkin, H. R. Meredith, J. K. Srimani, *et al.*, "Persistence and reversal of plasmid-mediated antibiotic resistance," *Nature Communications*, vol. 8, no. 1, pp. 1–10, 2017.
- [13] A. Prasetyoputri, A. M. Jarrad, M. A. Cooper, *et al.*, "The eagle effect and antibiotic-induced persistence: Two sides of the same coin?" *Trends in Microbiology*, vol. 27, no. 4, pp. 339–354, 2019.
- [14] R. F. Eyler and K. Shvets, "Clinical pharmacology of antibiotics," *Clinical Journal of the American Society of Nephrology*, vol. 14, no. 7, pp. 1080–1090, 2019.
- [15] B. Raymond, "Five rules for resistance management in the antibiotic apocalypse, a road map for integrated microbial management," *Evolutionary Applications*, vol. 12, no. 6, pp. 1079–1091, 2019.
- [16] R. Milo, P. Jorgensen, U. Moran, *et al.*, "Bionumbers—The database of key numbers in molecular and cell biology," *Nucleic Acids Research*, vol. 38, suppl. 1, pp. D750–D753, 2010.
- [17] D. Czock and F. Keller, "Mechanism-based pharmacokinetic-pharmacodynamic modeling of antimicrobial drug effects," *Journal of Pharmacokinetics and Pharmacodynamics*, vol. 34, no. 6, pp. 727–751, 2007.
- [18] J. Osuna, H. Viadiu, A. L. Fink, *et al.*, "Substitution of asp for ASN at position 132 in the active site of term Beta-lactamase: Activity toward different substrates and effects of neighboring residues," *Journal of Biological Chemistry*, vol. 270, no. 2, pp. 775–780, 1995.
- [19] A. J. Lee, S. Wang, H. R. Meredith, *et al.*, "Robust, linear correlations between growth rates and β -lactam-mediated lysis rates," *Proceedings of the National Academy of Sciences*, vol. 115, no. 16, pp. 4069–4074, 2018.
- [20] X. C. Wu, W. Lee, L. Tran, and S. L. Wong, "Engineering a bacillus subtilis expression-secretion system with a strain deficient in six extracellular proteases," *Journal of Bacteriology*, vol. 173, no. 16, pp. 4952–4958, 1991.
- [21] G. L. Drusano, "Role of pharmacokinetics in the outcome of infections," *Antimicrobial Agents and Chemotherapy*, vol. 32, no. 3, pp. 289–297, 1988.
- [22] G. Zlokarnik, P. A. Negulescu, T. E. Knapp, *et al.*, "Quantitation of transcription and clonal selection of single living cells with β -lactamase as reporter," *Science*, vol. 279, no. 5347, pp. 84–88, 1998.
- [23] K. M. Hallinen, J. Karlslake, and K. B. Wood, "Delayed antibiotic exposure induces population collapse in enterococcal communities with drug-resistant subpopulations," *Elife*, vol. 9, e52813, 2020.
- [24] B. Giwercman, E. T. Jensen, N. Høiby, *et al.*, "Induction of beta-lactamase production in pseudomonas aeruginosa biofilm," *Antimicrobial Agents and Chemotherapy*, vol. 35, no. 5, pp. 1008–1010, 1991.
- [25] R. Guilhaumou, S. Benaboud, Y. Bennis, *et al.*, "Optimization of the treatment with beta-lactam antibiotics in critically ill patients—guidelines from the French Society of Pharmacology and Therapeutics (Société Française de Pharmacologie et Thérapeutique—SFPT) and the French Society of Anaesthesia and Intensive Care Medicine (Société Française d'Anesthésie et Réanimation—SFAR)," *Critical Care*, vol. 23, no. 1, pp. 1–20, 2019.
- [26] M. Kılıç, N. Yüzkat, C. Soyalp, and N. Gülhaş, "Cost analysis on intensive care unit costs based on the length of stay," *Turkish Journal of Anaesthesiology and Reanimation*, vol. 47, no. 2, p. 142, 2019.
- [27] W. A. Craig, "Antimicrobial resistance issues of the future," *Diagnostic Microbiology and Infectious Disease*, vol. 25, no. 4, pp. 213–217, 1996.

Copyright © 2024 by the authors. This is an open access article distributed under the Creative Commons Attribution License ([CC BY-NC-ND 4.0](https://creativecommons.org/licenses/by-nc-nd/4.0/)), which permits use, distribution and reproduction in any medium, provided that the article is properly cited, the use is non-commercial and no modifications or adaptations are made.